J|A|C|S
ARTICLES
Published on Web 08/30/2003

Germanium and Tin Analogues of Alkynes and Their Reduction Products

Lihung Pu, Andrew D. Phillips, Anne F. Richards, Matthias Stender, Richard S. Simons, Marilyn M. Olmstead, and Philip P. Power*

Contribution from the Department of Chemistry, University of California, Davis, One Shields Avenue, Davis, California 95616

Received April 18, 2003; E-mail: pppower@ucdavis.edu

Abstract: The reduction of terphenylgermanium(II) or terphenyltin(II) chlorides with alkali metals was investigated. Treatment of Ar′GeCl or Ar*GeCl (Ar′ = C_6H_3-2,6-$Dipp_2$, Dipp = C_6H_3-2,6-Pr^i_2; Ar* = C_6H_3-2,6-$Trip_2$, Trip = C_6H_2-2,4,6-Pr^i_3) with lithium, sodium, or potassium afforded the neutral alkyne analogues Ar′GeGeAr′, **1**, Ar*GeGeAr*, **2**, the singly reduced radical species NaAr*GeGeAr*, **3**, or KAr′GeGeAr′, **4**, or the doubly reduced compounds Li_2Ar′GeGeAr′, **5**, Na_2Ar*GeGeAr*, **6**, or K_2Ar*GeGeAr*, **7**. Similarly, reduction of Ar′SnCl or Ar*SnCl afforded the neutral Ar′SnSnAr′, **8**, or Ar*SnSnAr*, **9**, the radical anions $[(THF)_3Na\{Ar^*SnSnAr^*\}]$, **10**, $[K(THF)_6][Ar'SnSnAr']$, **11**, $[K(THF)_6][Ar^*SnSnAr^*]$, **12**, $[K(18\text{-crown-6})(THF)_2][Ar^*SnSnAr^*]$, **13**, or the doubly reduced Na_2Ar*SnSnAr*, **14**, K_2Ar′SnSnAr′, **15**, or K_2Ar*SnSnAr*, **16**. The compounds were characterized by UV−vis, ^{1}H and ^{13}C NMR or EPR spectroscopy. The X-ray crystal structures of all compounds were determined except those of **2** and **9**. The neutral **1** and **8** displayed planar, trans-bent CMMC (M = Ge and Sn) cores with M−M−C angles of 128.67(8) and 125.24(7)°, respectively. The M−M bond lengths, 2.2850(6) and 2.6675(4)Å, indicated considerable multiple character and a bond order approaching two. Single and double reduction of the neutral species resulted in the narrowing of the M−M−C angles by ca. 12−32° and changes in the Ge−Ge and Sn−Sn bond lengths. One-electron reduction afforded a slight (ca. 0.03−0.05Å) lengthening of the Ge−Ge bonds in the case of germanium species **3** and **4** and a greater lengthening (ca. 0.13−0.15Å) for the Sn−Sn bonds in the tin compounds **10**−**13**. The addition of another electron yielded salts of the formal dianions $[Ar'MMAr']^{2-}$ and $[Ar^*MMAr^*]^{2-}$ which are isoelectronic to the corresponding doubly bonded, neutral arsenic and antimony derivatives. All the dianion salts were obtained as contact ion triples with two alkali metal cations complexed between aryl rings. The Ge−Ge bonds in the dianions of **5**−**7** were longer, whereas the Sn−Sn distances in the dianions in **14**, **15**, and **16** were shorter than those in the monoanions. Unusually, the Li_2Ar′GeGeAr′ salt, **5**, displayed a longer Ge−Ge bond (by ca. 0.06Å) than those of its Na^+ or K^+ analogue salts which was attributed to the greater polarizing power of Li^+. It was concluded that the M−M bond lengths in **3**−**7** and **10**−**16** are dependent on several factors that include M−M−C angle, Coulombic repulsion, alkali metal cation size, and the character of the molecular energy levels. The M−M bonding in the neutral compounds was accounted for in terms of a second-order Jahn−Teller mixing of σ^*- and a π-orbital which afforded bond orders near two for the neutral compounds, **1**, **2**, **8**, and **9**. Calculations on MeMMMe (M = Ge or Sn) model species showed that the LUMO corresponded to an orbital that had n_+ lone pair character. The slight Ge−Ge bond length increase upon one-electron reduction is consistent with these results, and the further bond lengthening upon double reduction is consistent with increased Coulombic repulsion. The greater Sn−Sn bond length increase seen for one-electron reduction of the tin species is probably due to the increased p-character of orbitals comprising the Sn−Sn σ-bond when the Sn−Sn−C angle is decreased by ca. 30°. Upon further reduction, the slight decrease in the Sn−Sn bond is probably a result of the reduced importance of Coulombic repulsion due to the larger size of tin and a widening of the Sn−Sn−C angles which may shorten the Sn−Sn σ-bond.

Introduction

The synthesis of stable heavier group 14 element analogues of alkynes has proven to be a considerable synthetic challenge[1,2] that has been partially overcome recently by the synthesis of germanium,[3] tin,[4] and lead[5] derivatives.[6] The synthesis and characterization of such compounds is of fundamental importance because of the enhanced understanding they provide on the bonding among such elements. In particular, the availability of stable heavier group 14 alkyne analogues allows the differences between the bonding in carbon and the heavier elements to be explored experimentally in a novel way. These

(1) Jutzi, P. *Angew. Chem., Int. Ed.* **2000**, *39*, 3797.
(2) Weidenbruch, M. *J. Organomet. Chem.* **2002**, *646*, 39.
(3) Stender, M.; Phillips, A. D.; Wright, R. J.; Power, P. P. *Angew. Chem., Int. Ed.* **2002**, *41*, 1785.
(4) Phillips, A. D.; Wright, R. J.; Olmstead, M. M.; Power, P. P. *J. Am. Chem. Soc.* **2002**, *124*, 5930.
(5) Pu, L.; Twamley, B.; Power, P. P. *J. Am. Chem. Soc.* **2000**, *122*, 3524.

10.1021/ja035711m CCC: $25.00

differences, which have their origin in the changing electronic structure of the atoms, are manifested in molecular energy patterns and structures that differ considerably from their lighter counterparts. Initial work in the area resulted in the synthesis of the singly reduced salts $[K(THF)_6][Ar^*SnSnAr^*]$, **12**, and $[K(18\text{-crown-6})(THF)_2][Ar^*SnSnAr^*]$, **13**, by reduction of Ar*SnCl with potassium.[7] The bulky terphenyl Ar* substituent ($Ar^* = C_6H_3\text{-}2,6\text{-}Trip_2$; $Trip = C_6H_2\text{-}2,4,6\text{-}Pr^i_3$)[8] was employed to stabilize both compounds. Later, the doubly reduced species $Na_2Ar^*GeGeAr^*$, **6**, and $K_2Ar^*SnSnAr^*$, **16**, were obtained by reaction of Ar*GeCl or Ar*SnCl for longer periods with excess alkali metal.[9] Both the singly and doubly reduced species featured a planar, trans-bent CMMC (M = Ge or Sn) core with M−M−C angles that did not exceed 107.50(14)°. Further work showed that the desired neutral species Ar*GeGeAr*, **2**,[10] and Ar*SnSnAr*, **9**, could also be isolated from these mixtures. Unfortunately, crystals of these compounds proved unsuitable for X-ray crystallography. Several different terphenyl ligands were investigated in order to overcome these crystallographic problems. Eventually, it was shown that use of the related Ar′ terphenyl substituent ($Ar' = C_6H_3\text{-}2,6\text{-}Dipp_2$; $Dipp = C_6H_3\text{-}2,6\text{-}Pr^i_2$) permitted a detailed examination of the structure of the first stable germanium and tin alkyne analogues Ar′GeGeAr′, **1**, and Ar′SnSnAr′, **8**.[3,4] We now present a more extensive and systematic examination of all three classes of compound in which we compare the effects of the ligands, alkali metal, and group 14 element on the M−M bonding. The bonding in the neutral alkyne analogues can be interpreted in terms of second-order Jahn−Teller $\sigma^*-\pi$-orbital mixing[11,12] which results in a diminution of the Ge−Ge and Sn−Sn bond orders from triple in an idealized linear geometry to approximately double in the more stable trans-bent geometries that are observed experimentally. The addition of one or two electrons to the neutral compounds to give singly or doubly reduced species results in relatively large changes to the trans-bending angles and M−M bond lengths. Different structural trends are found in the germanium and tin species which can be explained on the basis of the larger size and more electropositive character of the tin atom.

Experimental Section

General Procedures. All manipulations were carried out by using modified Schlenk techniques under an atmosphere of argon or N_2 or in a Vacuum Atmospheres HE-43 drybox. All solvents were distilled from molten Na/K alloy and degassed 3 times prior to use. The compounds LiAr′,[13] Ar*GeCl,[14] and Ar*SnCl[7,15] were prepared as previously described. ^{1}H, ^{13}C, and ^{119}Sn NMR spectra were recorded on Varian 300 and 400 spectrometers and referenced to known standards. UV−vis data were recorded on a Hitachi-1200 spectrometer, while infrared data were recorded as Nujol mulls using a Perkin-Elmer 1430 instrument. The EPR spectra **3** and **4** were obtained with use of a Bruker CWX band spectrometer operating near 9.6 GHz. Melting points were recorded using a Meltemp apparatus and are uncorrected.

$(Ar'GeCl)_2$ and $\{Ar'Sn(\mu\text{-}Cl)\}_2$. To a well stirred ether solution of $GeCl_2$(dioxane) (0.23 g, 1 mmol) at 0 °C was added LiAr′ (0.404 g, 1 mmol) in ether. The solution was allowed to warm to ambient temperature during which time it developed an orange color. Stirring was maintained for 12 h, after which time the solvents were removed under reduced pressure. The resultant orange powder was extracted into toluene and filtered. Storage of the solution at ca. −30 °C for 16 h afforded large orange crystals of $(Ar'GeCl)_2$ which were dried under reduced pressure. Yield: 74%, mp 150−155 °C (dec). ^{1}H NMR (399.8 MHz, 25 °C, C_6D_6): δ 0.99 (d, $^3J_{HH}$ = 6.81 Hz, 6H, *o*-CH(CH_3)$_2$), 1.29 (d, $^3J_{HH}$ = 6.81 Hz, 6H, *o*-CH(CH_3)$_2$), 2.72 (sept, $^3J_{HH}$ = 6.81 Hz, 8H, *o*-CH(CH$_3$)$_2$), 7.0−7.25 broad signal, aryl ring hydrogens. ^{13}C{^{1}H} NMR (100.5 MHz, 25 °C, C_6D_6): δ 22.72 (*o*-CH(CH_3)$_2$), 26.15 (*o*-CH(CH_3)$_2$), 31.02 (*o*-CH(CH$_3$)$_2$), 123.84 (*m*-Dipp), 128.59 (*p*-C_6H_3), 129.88 (*m*-C_6H_3), 130.85 (*i*-Dipp), 142.92 (*p*-Dipp), 145.97 (*o*-Dipp), 147.52 (*o*-C_6H_3), 167.54 (*i*-C_6H_3). In a similar manner, LiAr′ (4.85 g, 12 mmol) in Et_2O (40 mL) was added dropwise to a well stirred suspension of $SnCl_2$ (3.27 g, 17 mmol) in Et_2O (20 mL) with cooling in an ice bath. The reaction mixture became orange. Workup as above afforded orange crystals of the product $\{Ar'Sn(\mu\text{-}Cl)\}_2$ from toluene (50 mL) at ca. −25 °C. Yield: 5.75 g, 87%, mp 156−159 °C. ^{1}H NMR (399.8 MHz, 25 °C, C_6D_6): δ 1.03 (d, $^3J_{HH}$ = 6.80 Hz, 6H, *o*-CH(CH_3)$_2$), 1.31 (d, $^3J_{HH}$ = 6.80 Hz, 6H, *o*-CH(CH_3)$_2$), 3.06 (sept, $^3J_{HH}$ = 6.80 Hz, 4H, *o*-CH(CH$_3$)$_2$), 7.15 (s, 4H, *m*-Dipp), 7.24 (m, 4H, *p*-Dipp, *m*-C_6H_3), 7.27 (m, 1H, *p*-C_6H_3). ^{13}C{^{1}H} NMR (100.5 MHz, 25°C, C_6D_6): δ 23.47 (*o*-CH(CH_3)$_2$), 26.62 (*o*-CH(CH_3)$_2$), 31.54 (*o*-CH(CH$_3$)$_2$), 124.36 (*m*-Dipp), 128.18 (*p*-C_6H_3), 129.98 (*m*-C_6H_3), 131.08 (*i*-Dipp), 137.72 (*p*-Dipp), 145.76 (*o*-Dipp), 148.15 (*o*-C_6H_3), 181.95 (*i*-C_6H_3). ^{119}Sn{^{1}H} NMR (149.18 MHz, 25 °C, C_6D_6): δ 817.

Ar′GeGeAr′ (1) and Ar*GeGeAr* (2). At ambient temperature, a solution of Ar′GeCl (0.79 g, 1.56 mmol) in THF (10 mL) was added dropwise to finely divided potassium suspended in THF (30 mL) under vigorous stirring. After ca. 2 h, the reaction mixture began to turn red, and upon stirring for 56 h, the solution had become deep red. The THF was removed under reduced pressure, and the red solid residue was redissolved in hexane (30 mL). The potassium chloride precipitate and any remaining potassium was allowed to settle whereupon the supernatant solution was removed by decantation. The deep red solution was then concentrated to incipient crystallization (ca. 15 mL). Storage at 5 °C for 12 h yielded the product **1** as carmine/red-orange crystals. Yield: 0.28 g, 0.3 mmol, 39%, mp 214−216 °C (turns dark red/black after melting). ^{1}H NMR (C_6D_6, 399.77 MHz, 25 °C): δ 1.05 (d, $^3J_{H,H}$ = 6.8 Hz, 24H, *o*-CH(CH_3)$_2$), 1.30 (d, $^3J_{H,H}$ = 6.8 Hz, 24H, *o*-CH(CH_3)$_2$), 2.72 (sept, $^3J_{H,H}$ = 6.8 Hz, 8H, *o*-CH(CH$_3$)$_2$), 6.91 (d, $^3J_{H,H}$ = 7.2 Hz, 4H, *m*-C_6H_3), 7.09 (d, $^3J_{H,H}$ = 8.0 Hz, 8H, *m*-Dipp), 7.18 (t, $^3J_{H,H}$ = 7.2 Hz, 2H, *p*-C_6H_3), 7.29 (t, $^3J_{H,H}$ = 8.0 Hz, 4H, *p*-Dipp). ^{13}C{^{1}H} NMR (C_6D_6, 100.59 MHz, 25 °C): δ = 25.59 (*o*-CH(CH_3)$_2$), 26.06 (*o*-CH(CH_3)$_2$), 31.59 (*o*-CH(CH$_3$)$_2$), 124.58 (*m*-Dipp), 127.28 (*p*-C_6H_3), 130.024 (*m*-C_6H_3), 141.36 (*p*-Dipp), 145.67 (*i*-Dipp), 146.81 (*i*-C_6H_3), 147.29 (*o*-Dipp), 158.76 (*o*-C_6H_3). IR (Nujol): 1925(w), 1885(w), 1590(w), 1570(2), 1550(w), 1325(sh), 1055(m), 750(m), 450(w), 320(w) cm^{-1}. UV−vis (hexanes): λ_{max}, (ε, L mol^{-1} cm^{-1}): 501 nm (7500), 371 nm (34 000, sh), 280 nm (28000). In a similar manner,

(6) The existence of alkyne-like transient species such as MeSiSiMe,[a] 2,6-$Mes_2H_3C_6SiSiC_6H_3$-2,6-Mes_2,[b] R*SiSiR* (R* = $SiBu^t_3$),[c] (R_2*MeSi)SiSi(SiMeR_2*),[d] HCSiX (X = F or Cl),[e] and $Me_3SiCGeC_6H_3$-2,6($CH_2NPr^i_2$)$_2$[f] has been indicated by several experiments. In addition, the mono and dihydrogen bridged species $HSi(\mu\text{-}H)Si$[g] and $Si(\mu\text{-}H)_2Si$[h] have been structurally characterized by submillimeter spectroscopy. (a) Sekiguchi, A.; Zigler, S. S.; West, R. *J. Am. Chem. Soc.* **1986**, *108*, 4241. (b) Pietschnig, R.; West, R.; Powell, D. R. *Organometallics* **2000**, *19*, 2724. (c) Wiberg, N.; Finger, C. M. M.; Polborn, K. *Angew. Chem., Int. Ed. Engl.* **1993**, *32*, 1054. (d) Wiberg, N.; Niedermayer, W.; Fischer, G.; Nöth, H.; Sutin, M. *Eur. J. Inorg. Chem.* **2002**, 1066. (e) Karni, M.; Apeloig, Y.; Schröder, D.; Zummack, W.; Rabezzana, R.; Schwarz, H. *Angew. Chem., Int. Ed.* **1999**, *38*, 332. (f) Bibal, C.; Mazieres, S.; Gornitzka, C.; Couret, C. *Angew. Chem., Int. Ed.* **2001**, *40*, 952. (g) Cordonnier, M.; Bogey, M.; Demuynck, C.; Destombes, J. L. *J. Chem. Phys.* **1992**, *97*, 7984. (h) Bogey, M.; Bolvin, H.; Demuynck, C.; Destombes, J. L. *Phys. Rev. Lett.* **1991**, *66*, 413.

(7) Olmstead, M. M.; Simons, R. S.; Power, P. P. *J. Am. Chem. Soc.* **1997**, *119*, 11705.

(8) Twamley, B.; Haubrich, S. T.; Power, P. P. *Adv. Organomet. Chem.* **1999**, 441. Clyburne, J. A. C.; McMullen, N. *Coord. Chem. Rev.* **2000**, *210*, 73.

(9) Pu, L.; Senge, M. O.; Olmstead, M. M.; Power, P. P. *J. Am. Chem. Soc.* **1998**, *120*, 12682.

(10) Stender, M.; Phillips, A. D.; Power, P. P. *Chem. Commun.* **2002**, 1312.

(11) Bader, R. F. W. *Can. J. Chem.* **1962**, *40*, 1164.

(12) Grev, R. S. *Adv. Organomet. Chem.* **1991**, *33*, 125.

(13) Schiemenz, B.; Power, P. P. *Angew. Chem., Int. Ed. Engl.* **1996**, *35*, 2150.

(14) Pu, L.; Olmstead, M. M.; Power, P. P.; Schiemenz, B. *Organometallics* **1998**, *17*, 5602.

(15) Eichler, B. E.; Pu, L.; Stender, M.; Power, P. P. *Polyhedron* **2001**, *20*, 556.

reduction of Ar*GeCl (1.68 g, 2.85 mmol) in THF (60 mL) with potassium 0.112 g (2.85 mmol) at room temperature for 56 h, followed by standard work and recrystallization from hexane, afforded Ar*GeGeAr* **2** as red crystals. Yield: 0.55 g, 35%, 0.5 mmol, mp 244−246 °C (darkens above 200 °C, remains glassy after melting and cooling). Anal. Calcd for $C_{36}H_{49}Ge$: C 70.00, H 8.91. Found: C 78.36, H 8.80. ^{1}H NMR (C_6D_6): δ (ppm) 6.93 (s, 8H, *m*-Trip), 2.95 (sept, 4H, *p*-CH(CH_3)$_2$, ^3J = 6.8 Hz), 2.75 (sept, 4H, *o*-CH(CH_3)$_2$, ^3J = 6.8 Hz), 1.38 (d, 12H, *o*-CH(CH_3)$_2$, ^3J = 7.2 Hz), 1.30 (d, 12H, *o*-CH(CH_3)$_2$, ^3J = 7.2 Hz), 1.09 (d, 12H, *p*-CH(CH_3)$_2$, ^3J = 7.2 Hz). ^{13}C NMR (C_6D_6): δ (ppm) 156.8 (*i*-C_6H_3), 148.6 (*o*-C_6H_3), 146.1 (*o*-Trip), 139.1 (*p*-Trip), 128.6 (*i*-Trip), 128.2 (*m*-C_6H_3), 127.5 (*p*-C_6H_3), 121.7 (*m*-Trip), 34.6 (*p*-CH(CH_3)$_2$), 31.3 (*o*-CH(CH_3)$_2$), 25.7 (*o*-CH(CH_3)$_2$), 25.4 (*o*-CH(CH_3)$_2$), 24.4 (*o*-CH(CH_3)$_2$); UV−vis (toluene): λ_{max}, nm (ε, L mol^{-1} cm^{-1}) = 365 (31 000, sh), 490 (5500).

NaAr*GeGeAr* (3). An ice cold, green solution of sodium (0.042 g, 1.83 mmol) and naphthalene (0.24 g, 1.87 mmol) in THF (25 mL) was added dropwise to a rapidly stirred solution of Ar*GeCl (0.78 g, 1.32 mmol) in THF (10 mL) with cooling in a dry ice bath. The reaction mixture became red and was allowed to warm to room temperature. Upon stirring for 24 h, the solvent was stripped off and the residue was warmed (40 °C) under reduced pressure in the presence of a coldfinger to remove the naphthalene. The remaining solid was extracted with hexane (40 mL). The solution was allowed to settle, and the supernatant liquid was decanted. Reduction of the volume to ca. 20 mL under reduced pressure, and storage of the solution in a 6 °C refrigerator for several days, afforded the product **3** as orange-red crystals. Yield: 0.99 g, 0.58 mmol, 64%, mp 223−225 °C. Anal. Calcd for $C_{72}H_{88}Ge_2Na$: C, 76.41; H, 8.72. Found: C, 76.89; H, 8.98. UV−vis(hexane) λ_{max}, nm (ε, L mol^{-1} cm^{-1}): 703 (1400), 598 (1500).

KAr′GeGeAr′ (4). At room temperature, a THF (30 mL) solution of Ar′GeCl (1 mmol, 0.506 g) was added dropwise to a THF suspension of molten potassium (0.059 g, 1.5 mmol). Stirring was maintained until all the potassium was consumed, after which time the THF was removed under reduced pressure. The deep red colored powder was extracted into hexanes (50 mL), and the resultant dark red solution was filtered. Storage at ca. −20 °C for 24 h afforded the product **4** as red crystals suitable for X-ray crystallography. Anal. Calcd for $C_{60}H_{74}Ge_2K$: C 73.57, H 7.60. Found: C 72.1, H 7.61. UV−vis (benzene): λ_{max}, nm (ε, L mol^{-1} cm^{-1}): 698 (1500), 590 (1300). Yield: 0.152 g, 0.15 mmol, 31%, mp 74−76 °C.

Li$_2$Ar′GeGeAr′ (5). To a suspension of lithium powder (0.07 g, 10 mmol) in diethyl ether (10 mL) was added dropwise an ether solution of Ar′GeCl (0.54 g, 1 mmol) at room temperature. Immediately, the solution assumed a red color. After stirring for 16 h, the solution developed a deep brown color. Removal of the excess lithium by filtration and concentration of the ether solution afforded large dark red, almost black crystals of **5**. Yield: 0.10 g, 0.11 mmol, 21%, mp 171−173 °C. ^{1}H NMR (C_6D_6, 399.7 MHz, 25 °C): δ 1.052 (d, $^3J_{HH}$ = 6.8 Hz, 24H, *o*-CH(CH_3)$_2$), 1.241 (d, $^3J_{HH}$ = 6.8 Hz, 24H, *o*-CH(CH_3)$_2$), 2.824 (sept, $^3J_{HH}$ = 6.8 Hz, 18H, *o*-C*H*(CH_3)$_2$), 6.967 (d, $^3J_{HH}$ = 7.2 Hz, 4H, *m*-C_6H_3), 7.11 (d, $^3J_{HH}$ = 8.0 Hz, 8H, *m*-Dipp), 7.15 (t, $^3J_{HH}$ = 7.2 Hz, 4H, *p*-C_6H_3), 7.233 (t, J_{HH} = 8.0 Hz, 4H, *p*-Dipp). ^{13}C {^{1}H} NMR (C_6D_6, 100.59 MHz, 25 °C) δ 24.157 (*o*-CH(*C*H_3)$_2$), 23.271 (*o*-CH(*C*H_3)$_2$), 30.567 (*o*-CH(*C*H_3)$_2$), 122.667 (*m*-Dipp), 126.517 (*p*-C_6H_3), 131.251 (*m*-C_6H_3), 139.509 (*p*-Dipp), 146.610 (*i*-Dipp), 146.693 (*o*-Dipp), 148.292 (*o*-C_6H_3) (*i*-C_6H_3 carbon was not observed). ^{7}Li {^{1}H} NMR (C_6D_6), δ −2.206 (s). UV−vis (benzene): λ_{max}, nm (ε, L mol^{-1} cm^{-1}): 430 (3400), 570 (1500).

Na$_2$Ar*GeGeAr* (6). Ar*GeCl (1.29 g, 2.19 mmol) in benzene (20 mL) was added to finely divided sodium (0.30 g, 13.05 mmol) in benzene (10 mL) at room temperature with stirring. The reaction mixture was stirred for an additional 24 h at room temperature, and the resulting deep red solution was filtered. The filtrate was reduced to incipient crystallization (ca. 12 mL) under reduced pressure and stored in a ca. 6 °C refrigerator to yield the product **6** as red crystals. Yield: 0.38 g, 0.33 mmol, 30.1%, mp 234−236 °C. ^{1}H NMR (C_6D_6): δ 1.11 (d, 24H, $^3J_{HH}$ = 6.9 Hz, *p*-C*H*(CH_3)$_2$), 1.29 (d, 48H, $^3J_{HH}$ = 6.9 Hz, *o*-CH(CH_3)$_2$), 2.92 (sept, 4H, $^3J_{HH}$ = 6.9 Hz, *p*-C*H*(CH_3)$_2$), 3.60 (sept, 8H, $^3J_{HH}$ = 6.9 Hz, *o*-C*H*(CH_3)$_2$), 6.93 (m, 6H, *p*-C_6H_3, overlap), 7.04 (s, 8H, *m*-Trip). ^{13}C{^{1}H} NMR (C_6D_6): δ 23.67 (*o*-CH(*C*H_3)$_2$), 24.17 (*p*-CH(*C*H_3)$_2$), 25.56 (*o*-CH(*C*H_3)$_2$), 30.810 (*o*-*C*H(CH_3)$_2$), 34.15 (*p*-*C*H(CH_3)$_2$), 120.58 (*m*-Trip), 121.50 (*m*-C_6H_3), 128.52 (*o*-C_6H_3), 142.09 (*i*-Trip), 145.38 (*p*-C_6H_3), 147.27 (*p*-Trip), 148.32 (*o*-Trip), 176.16 (*i*-C_6H_3). λ_{max} (ε, L mol^{-1} cm^{-1}): 601 (1900), 464 (4200).

K$_2$Ar*GeGeAr* (7). Ar*GeCl (1.00 g, 1.70 mmol) in benzene (20 mL) was added to finely divided potassium (0.35 g, 8.95 mmol) in benzene (10 mL) at room temperature with stirring. The reaction mixture was stirred for an additional 24 h, and the resulting deep greenish-red solution was filtered. The filtrate was reduced to incipient crystallization (ca. 12 mL) and stored in a ca. 6 °C refrigerator to yield **7** as red crystals. Yield: 0.48 g, 0.40 mmol, 47%, mp 232−233 °C. ^{1}H NMR (C_6D_6): δ 1.13 (d, 24H, $^3J_{HH}$ = 6.8 Hz, *o*-CH(CH_3)$_2$), 1.17 (d, 24H, $^3J_{HH}$ = 6.8 Hz, *o*-CH(CH_3)$_2$), 1.32 (d, 24H, $^3J_{HH}$ = 6.8 Hz, *p*-CH(CH_3)$_2$) , 2.68 (sept, 4H, $^3J_{HH}$ = 6.8 Hz, *p*-C*H*(CH_3)$_2$), 3.78 (sept, 8H, $^3J_{HH}$ = 6.8 Hz, *o*-C*H*(CH_3)$_2$), 6.85−6.95 (mult, 6H, *m*, *p*-C_6H_3), 6.96 (s, 8H, *m*-Trip). ^{13}C {^{1}H} NMR (C_6D_6): δ 24.26 (*o*-CH(*C*H_3)$_2$), 24.61 (*p*-CH(*C*H_3)$_2$), 25.00 (*o*-CH(*C*H_3)$_2$), 30.85 (*o*-*C*H(CH_3)$_2$), 34.49 (*p*-*C*H(CH_3)$_2$), 120.64 (*m*-Trip), 120.81 (*m*-C_6H_3), 129.15 (*o*-C_6H_3), 142.68 (*i*-Trip), 147.44 (*p*-C_6H_3), 147.54 (*p*-Trip), 149.65 (*o*-Trip), 177.63 (*i*-C_6H_3). UV−vis (hexane) λ_{max} (ε, L mol^{-1} cm^{-1}): 605 (1700), 470 (4600).

Ar′SnSnAr′ (8) and Ar*SnSnAr* (9). A benzene solution (50 mL) of Ar′SnCl (1.21 g, 2.2 mmol) was added dropwise to finely divided potassium (0.086 g, 2.2 mmol) in benzene (10 mL) at room temperature. The reaction mixture was stirred for 3 days, after which time the precipitate was allowed to settle for 4 h. The intensely dark blue-green solution was decanted from the precipitated solid. The volume of the solution was reduced to incipient crystallization and stored in a ca. 6 °C refrigerator to give the product **1** as purple crystals. Yield: 0.31 g, 0.30 mmol, 32.2%. mp 208−10 °C (dec). UV−vis (hexanes) λ_{max} (ε, L mol^{-1} cm^{-1}) 410 (2000), 597 (1700). ^{1}H NMR (C_6D_6, 399.77 MHz, 25 °C): δ 1.13 (d, 24H, ^3J = 6.0 Hz, *o*-CH(CH_3)$_2$), 1.39 (d, 24H, ^3J = 6.0 Hz, *o*-CH(CH_3)$_2$), 2.87 (sept, 8H, ^3J = 6.0 Hz, *o*-C*H*(CH_3)$_2$), 6.22 (t, 2H, ^3J = 7.2 Hz, *p*-C_6H_3), 7.05 (d, 8H, ^3J = 7.2 Hz, *m*-Dipp), 7.19 (t, 4H, ^3J = 7.2 Hz, *p*-Dipp), 7.51 (d, 4H, ^3J = 7.2 Hz, *m*-C_6H_3). ^{13}C {^{1}H} NMR (C_6D_6, 100.53 MHz, 25 °C): δ 27.44 (*o*-CH(*C*H_3)$_2$), 32.67 (*o*-CH(*C*H_3)$_2$), 34.98 (*o*-*C*H(CH_3)$_2$), 124.55 (*p*-C_6H_3), 125.94 (*m*-Dipp), 130.65 (*m*-C_6H_3), 131.68 (*i*-Dipp), 141.72 (*p*-Dipp), 150.84 (*o*-Dipp), 153.98 (*i*-C_6H_3), 159.02 (*o*-C_6H_3). ^{119}Sn NMR (C_6D_6, 149.00 MHz, 25 °C): δ no signal observed. In a similar manner, Ar*SnCl (1.202 g, 1.89 mmol) in toluene (50 mL) was added to a stirred suspension of finely divided potassium (0.078 g, 2 mmol) in toluene (25 mL) at room temperature. The solution was stirred for 3 d during which time the color changed to dark greenish blue. The mother liquor was decanted from the settled precipitates, and the volume was reduced to ca. 20 mL. Storage of the solution at −25 °C for 1 week resulted in deposition of very air and moisture sensitive dark blue-green crystals of **9**. Anal. Calcd for $C_{36}H_{49}Sn$: C, 72.00; H, 8.22. Found: C, 72.91; H, 8.41. Yield: 42%, 0.480 g, 0.40 mmol,, mp 134−138 °C (dec) to red solid. UV−vis (hexane) λ_{max} (ε, L mol^{-1} cm^{-1}) 409 (1800), 593 (1400). ^{1}H NMR (399.8 MHz, 25 °C, C_6D_6) δ 1.14 (d, $^3J_{HH}$ = 6.4 Hz, *o*-CH(CH_3)$_2$), 1.15 (d, $^3J_{HH}$ = 6.4 Hz, *o*-CH(CH_3)$_2$), 1.23 (d, $^3J_{HH}$ = 6.4 Hz, *o*-CH(CH_3)$_2$), 1.30 (d, $^3J_{HH}$ = 6.2 Hz, *p*-CH(CH_3)$_2$), 2.84 (sept, $^3J_{HH}$ = 6.4 Hz, *o*-C*H*(CH_3)$_2$), 2.96 (sept, $^3J_{HH}$ = 6.4 Hz, *o*-C*H*(CH_3)$_2$), 3.05 (sept, $^3J_{HH}$ = 6.2 Hz, *p*-C*H*(CH_3)$_2$), 3.97 (t, $^3J_{HH}$ = 7.6 Hz, *p*-C_6H_3), 7.00 (s, *m*-Trip), 8.65 (d, $^3J_{HH}$ = 7.6 Hz, *m*-C_6H_3). ^{13}C{^{1}H} NMR (100.5 MHz, 25°C, C_6D_6) δ 23.06 (*o*-CH(*C*H_3)$_2$), 24.66 (*o*-CH(*C*H_3)$_2$), 28.05 (*p*-CH(*C*H_3)$_2$), 29.45 (*p*-*C*H(CH_3)$_2$), 32.49 (*o*-*C*H(CH_3)$_2$), 112.54 (*p*-C_6H_3), 119.35 (*m*-C_6H_3), 122.84 (*m*-Trip), 145.45 (*o*-C_6H_3), 147.02 (*i*-Trip), 149.80 (*o*-Trip), 155.96 (*p*-Trip), 188.84 (*i*-Trip), 188.84 (*i*-C_6H_3). ^{119}Sn{^{1}H} NMR (149.51 MHz, 25 °C, C_6D_6) δ no signal observed.

[(THF)$_3$Na{Ar*SnSnAr*}] (10). An ice-cold, blue solution of sodium (0.031 g, 1.35 mmol) and anthracene (1.35 mmol, 0.178 g) in THF (35 mL) was added dropwise to a rapidly stirred solution of Ar*SnCl (0.84 g, 1.32 mmol) in THF (20 mL) which was cooled in a dry ice bath. The reaction mixture became orange-brown and was allowed to warm to room temperature. Upon stirring for 24 h, the solvents were stripped off and the residue was warmed (50 °C) under reduced pressure for 20 h in the presence of a coldfinger to remove the anthracene. The remaining material was extracted with pentane (40 mL). The solution was allowed to settle and the supernatant liquid was filtered through Celite. Reduction of the volume to ca. 20 mL under reduced pressure, and storage of the solution in a ca. −20 °C freezer for several days afforded the product **2** as orange-red crystals. Yield: 0.35 g, 36%. Calcd for $C_{84}H_{122}NaO_3Sn_2$: C, 70.05, H, 8.54. Found: C = 70.96, H = 8.19. UV−vis(hexane) λ_{max}, nm (ε, L mol^{-1} cm^{-1}): 709 (140).

[K(THF)$_6$][Ar′SnSnAr′] (11). A dark green solution of Ar′SnSnAr′ (**8**) (1.033 g, 1 mmol) in THF (50 mL) was added to a suspension of finely divided potassium (0.196 g, 5 mmol). The solution was stirred for 2 d by which time the color had darkened slightly. The suspended excess potassium and KCl were allowed to settle, and the solution was decanted and reduced in volume to incipient crystallization. Storage in a ca. −25 °C freezer yielded the product **11**·THF as highly air and moisture sensitive dichroic green-orange crystals. Yield: 0.504 g, 0.32 mmol, 32%, mp 152−164 °C (dec). Anal. Calcd for $C_{84}H_{122}KO_6Sn_2$: C, 67.06; H 8.18. Found: C, 68.01; H 8.23. UV−vis (THF) λ_{max}, nm (ε, L mol^{-1} cm^{-1}): 461 (1900).

[K(THF)$_6$][Ar*SnSnAr*] (12) and [K(12-crown-6)(THF)$_2$][Ar*-SnSnAr*] (13). Ar*SnCl (1.00 g, 1.57 mmol) and KC_8 (0.21 g, 1.54 mmol) in THF (20 mL) were stirred rapidly at room temperature for 2 h. All volatile materials were removed under reduced pressure, and the residue was extracted with a THF/toluene, 3:1 mixture (30 mL) and rapidly filtered through Celite. The dark red solution was concentrated to incipient crystallization and stored in a ca. −20 °C freezer for 2 days to afford the product **12** as orange-green dichroic crystals. Yield: 0.36 g, 0.22 mmol, 27%, mp 120 °C (dec). Anal. Calcd for $C_{96}H_{146}KO_6Sn_2$: C, 68.92; H, 8.80. Found C, 68.13; H, 8.97. The compound **13**·2THF was obtained similarly except that dibenzo-18-crown-6 was included in the reaction mixture. The product **13**·2THF was obtained in 22% yield, mp 125 °C (dec).

Na$_2$Ar*SnSnAr* (14). In a manner similar to the preparation of **6**, Ar*SnCl (2.00 g, 3.14 mmol) in benzene (40 mL) was added to finely divided sodium (0.50 g, 21.75 mmol) in benzene (10 mL). The solution was stirred for 24 h and filtered to afford a dark red, almost black solution which was reduced to incipient crystallization (ca. 25 mL). Storage in a ca. 6 °C refrigerator for 24 h afforded **14** as red crystals. Yield: 1.65 g, 37.1%. ^{1}H NMR (C_6D_6, 17.6 °C): δ 1.13 (d, 6H, $^3J_{HH}$ = 6.6 Hz, *o*-CH(CH_3)$_2$), 1.19 (d, 6H, $^3J_{HH}$ = 4.5 Hz, *o*-CH(CH_3)$_2$), 1.21 (d, 6H, $^3J_{HH}$ = 4.5 Hz, *o*-CH(CH_3)$_2$), 1.28 (d, 12H, $^3J_{HH}$ = 6.9 Hz, *p*-CH(CH_3)$_2$), 1.35 (d, 6H, $^3J_{HH}$ = 6.9 Hz, *o*-CH(CH_3)$_2$), 2.97 (sept, 8H, $^3J_{HH}$ = 7.2 Hz, *o*-CH(CH$_3$)$_2$), 3.59 (br, 4H, *p*-CH(CH$_3$)$_2$), 6.91−7.20 (mult, 10H, aromatic region).

K$_2$Ar′SnSnAr′ (15) and K$_2$Ar*SnSnAr* (16). A solution of Ar′SnSnAr′ (**8**) (1.033 g, 1 mmol) in benzene (30 mL) was added dropwise to a suspension of finely divided potassium (0.469 g, 12 mmol). The solution was stirred for 5 days, by which time the color had changed from dark green to dark red. The suspended solids were allowed to settle, and the supernatant solution was decanted and reduced in volume to incipient crystallization. Storage at room temperature for 4 h yielded the product as highly air and moisture sensitive dark red crystals. Yield: 26%, 0.289 g, 0.26 mmol, mp 141−163 °C (dec). UV−vis(benzene) λ_{max}, nm (ε, L mol^{-1} cm^{-1}): 408 (3900), 556 (2200), 875 (152). ^{1}H (399.8 MHz, 25 °C, C_6D_6): δ 0.970 (d, $^3J_{HH}$ = 6.80 Hz, 12H, *o*-CH(CH_3)$_2$), 0.984 (d, $^3J_{HH}$ = 6.80 Hz, 12H, *o*-CH(CH_3)$_2$), 2.75 (sept, $^3J_{HH}$ = 6.80 Hz, 4H, *o*-CH(CH$_3$)$_2$), 6.91 (d, $^3J_{HH}$ = 7.60 Hz, 8H, *m*-Dipp), 7.02 (t, $^3J_{HH}$ = 8.00 Hz, 2H, *p*-C_6H_3), 7.06 (d, $^3J_{HH}$ = 8.00 Hz, 4H, *m*-C_6H_3), 7.15 (t, $^3J_{HH}$ = 7.60 Hz, 4H, *p*-Dipp). ^{13}C{^{1}H} NMR (100.5 MHz, 25 °C, C_6D_6): δ 24.18 (*o*-CH(*C*H$_3$)$_2$), 24.30 (*o*-CH(*C*H$_3$)$_2$), 30.60 (*o*-*C*H(CH$_3$)$_2$), 122.71 (*m*-Dipp), 128.26 (*p*-Dipp), 133.28 (*m*-C_6H_3), 134.24 (*p*-C_6H_3), 139.54 (*i*-Dipp), 140.93 (*o*-C_6H_3), 146.71 (*o*-Dipp), not observed (*i*-C_6H_3). ^{119}Sn{^{1}H} NMR (149.53 MHz, 25 °C, C_6H_6): δ no signal observed. In a manner similar to the synthesis of **15**, **7** (1.2 g, 1.9 mmol) in benzene (20 mL) was added to finely divided potassium (0.45 g, 11.4 mmol) in benzene (10 mL) at room temperature and stirred for 16 h. The dark red solution was evaporated to dryness, and the residue was extracted with toluene (40 mL) and filtered. The filtrate was reduced to incipient crystallization (ca. 15 mL) and stored in a ca. 6 °C refrigerator to yield **16** as dark red crystals. Yield: 0.43 g, 30%, mp 228−230 °C. ^{1}H NMR (C_6D_6, 60 °C): δ 1.02 (d, 6H, $^3J_{HH}$ = 6.9 Hz, *p*-CH(CH_3)$_2$), 1.11 (d, 6H, $^3J_{HH}$ = 6.9 Hz, *p*-CH(CH_3)$_2$), 1.16 (d, 6H, $^3J_{HH}$ = 6.9 Hz, *p*-CH(CH_3)$_2$), 1.19 (d, 6H, $^3J_{HH}$ = 6.6 Hz, *o*-CH(CH_3)$_2$), 1.30 (d, 6H, $^3J_{HH}$ = 6.9 Hz, *o*-CH(CH_3)$_2$), 1.41 (d, 6H, $^3J_{HH}$ = 6.9 Hz, *o*-CH(CH_3)$_2$), 2.76 (sept, 1H, $^3J_{HH}$ = 6.9 Hz, *o*-CH(CH$_3$)$_2$), 2.89 (sept, 1H, $^3J_{HH}$ = 6.9 Hz, *o*-CH(CH$_3$)$_2$), 2.92 (sept, 2H, $^3J_{HH}$ = 6.9 Hz, *p*-CH(CH$_3$)$_2$), 3.06 (sept, 1H, $^3J_{HH}$ = 6.9 Hz, *o*-CH(CH$_3$)$_2$), 3.24 (sept, 1H, $^3J_{HH}$ = 6.9 Hz, *o*-CH(CH$_3$)$_2$), 6.82 (t, 1H, $^3J_{HH}$ = 3.2 Hz, *p*-C_6H_3). ^{13}C {^{1}H} NMR (C_6D_6): δ 23.83 (*o*-CH(*C*H$_3$)$_2$), 24.43 (*p*-CH(*C*H$_3$)$_2$), 24.57 (*o*-CH(*C*H$_3$)$_2$), 25.75 (*p*-CH(*C*H$_3$)$_2$), 30.63 (*o*-CH(CH$_3$)$_2$), 34.24 (*p*-*C*H(CH$_3$)$_2$), 34.98 (*o*-*C*H(CH$_3$)$_2$), 120.49 (*m*-Trip), 130.42, 132.22 (*m*-C_6H_3), 141.45, 141.51 (*o*-C_6H_3), 146.62, 146.98 (*i*-Trip), 147.07, 147.22 (*p*-C_6H_3), 148.35, 148.44 (*o*-Trip), 150.18 (*p*-C_6H_3), 169.80 (*i*-C_6H_3). UV−vis (toluene) λ_{max}, nm (ε, L mol^{-1} cm^{-1}): 552 (3200), 412 (4200).

X-ray Crystallographic Studies. The samples were prepared by removing the crystal from the Schlenk tube under a rapid flow of Argon and immediately submerging it in hydrocarbon oil. A suitable crystal was selected, mounted on a glass fiber attached to a copper pin, and rapidly placed in the cold stream of N_2 of the diffractometer for data collection.[16] Data were collected at 90 K (Ar′GeCl, Ar′SnCl, **4**, **5**, **15**) on a Bruker SMART 1000 diffractometer or at 140 K (**11** and **14**) on a Simens R3m/V with use of Mo Kα (λ = 0.710 73Å) radiation and a CCD area detector. Data for **3** and **7** were collected at 130 K on a Siemens R3m/V diffractometer with Cu Kα (λ = 1.541 78Å) radiation. Empirical absorption corrections were applied using SADABS[17a] or XABS (**3**, **7**, **11**, **14**).[17b] The crystal structures were solved with use of either direct methods or the Patterson option in SHELXS[18] and refined by the full-matrix least-squares procedure in SHELXL.[18] All non-hydrogen atoms were refined anisotropically while hydrogens were placed at calculated positions and included in the refinement using a riding model. A number of the structures, (Ar′GeCl)$_2$·PhMe, **3**·0.5hexane, **11**·2THF, **14**·3C_6H_6, and **15**·1.5C_6H_6 contained disordered solvent molecules which could be satisfactorily refined with use of partial occupancies. Hydrogen atoms were not added to these molecules. Some details of the data collection and refinement are given in Table 1. Further details are in the Supporting Information.

Results and Discussion

Precursors. Ar′MCl (M = Ge or Sn). All compounds discussed in this paper are derivatives of the sterically crowded terphenyl ligands Ar′ and Ar* as illustrated by

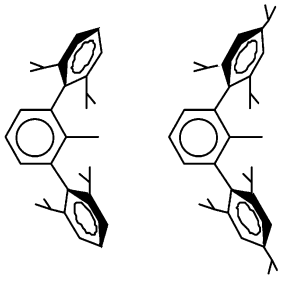

Table 1. Selected Crystallographic Data for Compounds (Ar′GeCl)$_2$, {Ar′Sn(μ-Cl)}$_2$, **3**−**5**, **7**, **11**, **14**, and **15**

compd	(Ar′GeCl)$_2$·PhMe	{Ar′Sn(μ-Cl)}$_2$	NaAr*GeGeAr*·0.5hexane (**3**·0.5 hexane)	KAr′GeGeAr′ (**4**)	Li$_2$Ar′GeGeAr′ (**5**)	K$_2$Ar*GeGeAr*·4C$_6$H$_6$ (**7**·4C$_6$H$_6$)	[K(THF)$_6$][Ar′SnSnAr′] 2THF (**11**·2THF)	Na$_2$Ar*SnSnAr*·3C$_6$H$_6$ (**14**·3C$_6$H$_6$)	K$_2$Ar′SnSnAr′·1.5C$_6$H$_6$ (**15**·1.5C$_6$H$_6$)
formula	$C_{67}H_{82}Cl_2Ge_2$	$C_{60}H_{74}Cl_2Sn_2$	$C_{75}H_{105}Ge_2Na$	$C_{60}H_{74}Ge_2K$	$C_{60}H_{74}Ge_2Li_2$	$C_{96}H_{122}Ge_2K_2$	$C_{88}H_{130}KO_8Sn_2$	$C_{90}H_{116}Na_2Sn_2$	$C_{78}H_{92}K_2Sn_2$
fw	1103.41	1103.47	1174.81	979.47	954.25	1499.32	1592.40	1481.19	1345.10
color, habit	orange, block	orange, block	red/green dichroic, needle	red/brown, block	dark red, block	black, block	orange green, block	red, bipyramids	dark red, block
cryst syst	monoclinic	monoclinic	monoclinic	monoclinic	triclinic	triclinic	monoclinic	tetragonal	monoclinic
space group	*C*2/*c*	*P*2$_1$/*n*	*P*2$_1$/*n*	*P*2$_1$/*c*	*P*$\bar{1}$	*P*$\bar{1}$	*C*2/*m*	*P*4$_3$2$_1$2	*C*2/*c*
a, Å	27.411(2)	13.3297(7)	14.2725(15)	10.6822(13)	9.617(2)	12.5633(13)	17.433(2)	16.720(4)	26.268(2)
b, Å	14.0940(8)	14.1189(9)	20.169(2)	19.393(2)	12.705(3)	12.8465(12)	18.014(3)	16.720(4)	18.7851(16)
c, Å	15.5937(9)	14.4249(10)	24.160(2)	26.455(3)	12.833(4)	15.1597(11)	14.4750(18)	29.616(6)	15.0562(13)
α, °					113.680(5)	81.996(7)			
β, °	104.125(2)	97.247(3)	98.192(8)	93.599(2)	97.789(9)	74.240(7)	96.551(4)		111.697(2)
γ, °					110.46(2)	65.170(7)			
V, A^3	5842.1(6)	2693.1(3)	6884.0(12)	5469.7(11)	2547.6(12)	2136.2(3)	4516.0(10)	8279(3)	6903.2(10)
Z	4	2	4	4	1	1	2	4	4
cryst dims, mm^3	0.41 × 0.41 × 0.34	0.52 × 0.41 × 0.32	0.54 × 0.20 × 16	0.41 × 0.35 × 0.28	0.34 × 0.41 × 0.13	0.40 × 0.40 × 0.40	0.32 × 0.21 × 0.18	0.24 × 0.22 × 0.20	0.17 × 0.15 × 0.05
d calc, g cm^{-3}	1.255	1.361	1.134	1.189	1.244	1.165	1.171	1.188	1.294
μ, mm^{-1}	1.160	1.063	1.414	1.210	1.217	2.055	0.648	0.655	0.885
no. of rflns	9280	4946	8969	10685	4995	5640	4194	5429	6218
no. of obsd rflns	7545	4240	7064	9047	3896	5140	3489	3387	5599
R, obsd rflns	0.0356	0.0697	0.0479	0.0371	0.0486	0.0376	0.0546	0.0604	0.0242
wR$_2$, all	0.0957	0.1997	0.1159	0.0983	0.1174	0.0994	0.1750	0.1122	0.0617

The synthesis of compounds **1**−**16** involved the reduction of the aryl element halide precursors Ar′MCl or Ar*MCl (M = Ge or Sn) with an alkali metal. The synthesis and properties of the precursors Ar*MCl (M = Ge[14] or Sn[15]) have been described previously. The Ar′MCl species were synthesized in a similar manner by the straightforward reaction of 1 equiv of LiAr′[13] with $GeCl_2$·dioxane or $SnCl_2$. They were isolated as orange crystals and have physical properties similar to their Ar* substituted analogues. Their structures, however, show unexpected differences which can be attributed to the slightly smaller size of the Ar′ ligand. Ar′GeCl crystallizes from toluene as Ge−Ge bonded dimers (Ar′GeCl)$_2$ as illustrated in Figure 1. The structure has a centrosymmetric, trans-pyramidal ClCGeGeCCl core with Ge(1)−Ge(1A), Ge(1)−C(1), and Ge(1)−Cl(1) distances of 2.4624(4), 1.976(2), and 2.2167(5) Å, respectively. The Ge−Ge bond length may be compared with those previously published for (Ar*GeCl)$_2$ (Ge−Ge = 2.363(2) Å)[14] and (2,6-$Mes_2H_3C_6$GeCl)$_2$ (Ge−Ge = 2.443(2) Å).[19] Unexpectedly, the Ge−Ge distance in the Ar′GeCl dimer is the longest of the three compounds. Furthermore, the coordination geometry at germanium is the most pyramidal ($\Sigma°$ Ge = 327.82°), and the out-of-plane angle (38.8°, i.e., the angle between the Ge−Ge bond and the GeCCl plane) is very similar to the 39.0° in the least crowded derivative 2,6-$Mes_2H_3C_6$GeCl. As in the structure of 2,6-$Mes_2H_3C_6$GeCl,[19] part of the explanation of the long Ge−Ge distance lies in the relatively close contacts between germanium and a flanking aryl ring (e.g., C(6) (2.822 Å), C(7) (2.984 Å)) which effectively increase the germanium coordination number. Such interactions can occur in aryl group 14 element(II) halide derivatives owing to less crowding Ar′ and C_6H_3-2,6-Mes_2 [5] ligands and enhanced Lewis acidity conferred by the halogen coligand. The interactions are prevented in (Ar*GeCl)$_2$ by the para Pr^i groups on the flanking rings which cause steric conflict that disfavors close Ge··C approaches. The unusual circumstance whereby para-Pr^i substituents can exert a steric effect may also be understood from structures such as **8** and **11** (Figure 1) where, because of configuration of the terphenyl groups within the molecules, para Pr^i groups, if they were present, would be oriented toward each other (see also the structures of the lithium salts of Ar′ and Ar* for structural differences due to the absence of para Pr^i groups).[13,14]

The Ar′SnCl precursor also has a dimeric structure, {Ar′Sn(μ-Cl)}$_2$, which, like {Ar*Sn(μ-Cl)}$_2$, has tins that are bridged by chlorines. However, the bridging distances in [Ar′Sn(μ-Cl)]$_2$ are significantly longer than those observed for {Ar*Sn(μ-Cl)}$_2$. The latter has almost equal Sn−Cl distances (2.5768(6) and 2.5978(7) Å) in the Sn_2Cl_2 core, whereas the corresponding distances in {Ar′Sn(μ-Cl)}$_2$ are significantly longer at 2.651(1) and 2.967(1) Å. As in the germanium structure, part of the explanation for the weaker association of the Ar′SnCl monomers in close contacts between the tin and carbons (e.g., C(7) (2.999(6) Å) and C(2) (3.014(6) Å)) of a flanking aryl ring which effectively increase the tin coordination number and weaken the already feeble association even further. The compound exists as a monomer in hydrocarbon solution as indicated by the ^{119}Sn

(16) Hope, H. *Prog. Inorg. Chem.* **1995**, *41*, 1.
(17) (a) *SADABS: Area-Detector Absorption Corrections*; Bruker AXS Inc.: Madison, WI, 1996. (b) *XABS*: Parkin, S.; Moezzi, B.; Hope, H. *J. Appl. Crystallogr.* **1995**, *28*, 53.
(18) *SHELXLPC*, version 5.03; Bruker AXS Inc.: Madison, WI, 1994.
(19) Simons, R. S.; Pu, L.; Olmstead, M. M.; Power, P. P. *Organometallics* **1997**, *16*, 1920.

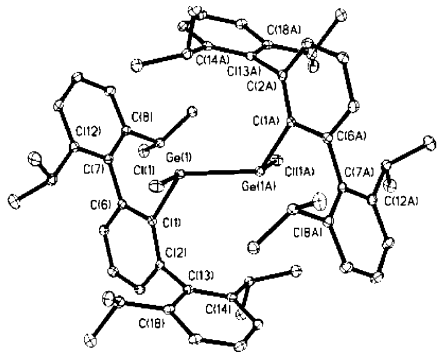

Ar'GeCl

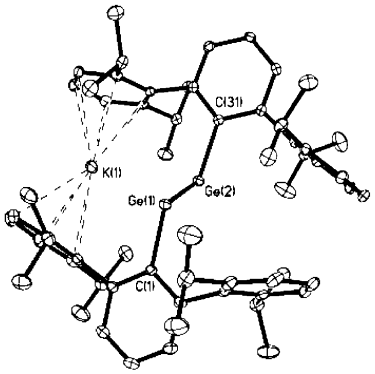

4

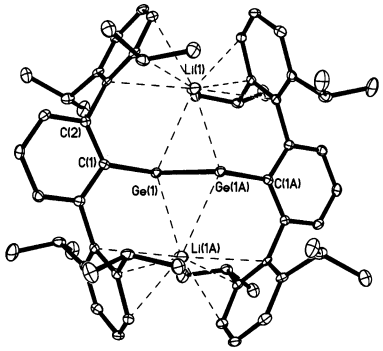

5

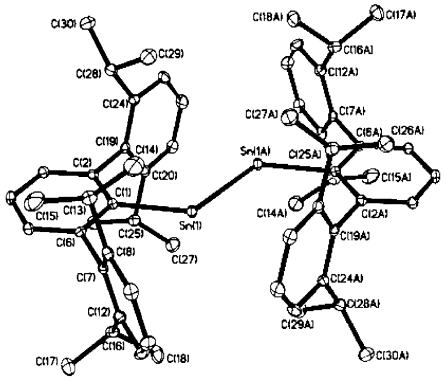

8

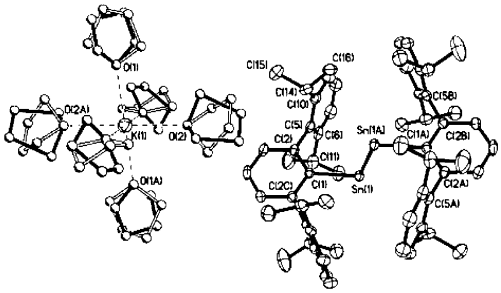

11

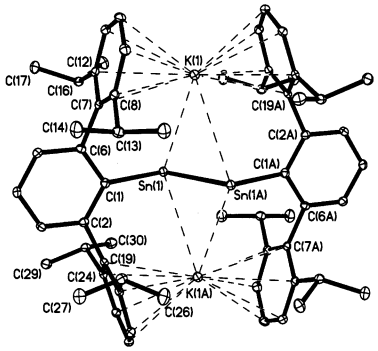

15

Figure 1. Thermal ellipsoid (30%) drawings of the representative structures $(Ar'GeCl)_2$, KAr′GeGeAr′ (**4**), $Li_2Ar'GeGeAr'$ (**5**), Ar′SnSnAr′ (**8**), $[K(THF)_6][Ar'SnSnAr']$ (**11**), $K_2Ar'SnSnAr'$ (**15**). Selected bond distances and angles for these compounds and $\{Ar'Sn(\mu\text{-}Cl)\}_2$, **1**, **3**, **6**, **7**, **10**, **12**−**14**, and **16** are given in Tables 2, 4, and 5.

NMR chemical shift of 817 ppm which is very similar to the 793.4 ppm observed for Ar*SnCl.[15]

Neutral Ar′MMAr′ and Ar*MMAr* (M = Ge or Sn). The original objective in the reduction of the Ar′MCl and Ar*MCl (M = Ge or Sn) aryl element halides by alkali metals was the isolation of stable germanium and tin analogues of alkynes. Initially, however, salts containing the tin radical monoanion $[Ar*SnSnAr*]^{\bullet-}$ were crystallized with several different countercations (see below),[7] and later, the doubly reduced dianionic salts $K_2Ar*GeGeAr*$, **7**, and $Na_2Ar*SnSnAr*$, **16**, were isolated.[8] Experiments with stoichiometric quantities of alkali metal reductant (i.e., a 1:1 ratio of alkali metal:Ar*MCl) showed that the "overreduced" mono- and dianions were produced in addition to the neutral species, especially if short (<ca. 4 h) reaction times were used. The amounts of the charged species can be minimized, and almost eliminated, by the use of exactly stoichiometric quantities of alkali metal and stirring for extended periods (2−3 days). In this way, the desired neutral germanium and tin alkyne analogues **1**, **2**, **8**, and **9** could be crystallized. At first, all experiments were carried out with use of the Ar* substituent,[20] and X-ray quality crystals of Ar* substituted derivatives could be obtained for the mono- and dianions in a relatively straightfoward manner. But the neutral Ar*GeGeAr*, **2**,[10] and Ar*SnSnAr*, **9**,[4] although they appeared to crystallize well, displayed poor diffraction characteristics and did not extinguish under polarized light. Experiments with various bulky terphenyl ligands showed that the use of the related Ar′ ligand, which differs from Ar* only in that it does not carry para-Pr^i

(20) Schiemenz, B.; Power, P. P. *Organometallics* **1996**, *15*, 958.

Table 2. Selected Bond Distances (Å) and Angles (deg) for $(Ar'GeCl)_2$, $\{Ar'Sn(\mu\text{-}Cl)\}_2$, Ar′GeGeAr′ (**1**), and Ar′SnSnAr′ (**8**)

$\{Ar'GeCl\}_2$		$\{Ar'Sn(\mu\text{-}Cl)\}_2$	
Ge(1)−Ge(1A)	2.4624(4)	Sn(1)−C(1)	2.225(6)
Ge(1)−C(1)	1.9758(17)	Sn(1)−Cl(1)	2.650(1)
Ge(1)−Cl(1)	2.2167(5)	Sn(1)−Cl(1A)	2.967(1)
C(1)−Ge(1)−Cl(1)	102.51(5)	C(1)−Sn(1)−Cl(1)	91.14(7)
C(1)−Ge(1)−Ge(1A)	119.51(5)	Sn(1)−C(1)−C(2)	109.9(5)
Cl(1)−Ge(1)−Ge(1A)	105.80(2)	Sn(1)−C(1)−C(6)	131.6(5)
Ge(1)−C(1)−C(6)	111.7(1)	C(2)−C(1)−C(6)	118.5(6)
Ge(1)−C(1)−C(6)	128.5(1)		
C(2)−C(1)−C(6)	119.8(2)		
Ar′GeGeAr′ (1)		**Ar′SnSnAr′ (8)**	
Ge(1)−Ge(1A)	2.2850(8)	Sn(1)−Sn(1A)	2.6675(4)
Ge(1)−C(1)	1.996(3)	Sn(1)−C(1)	2.191(3)
Ge(1)−Ge(1A)−C(1A)	128.67(8)	Sn(1)−Sn(1A)−C(1A)	125.24(7)
Ge(1)−C(1)−C(2)	116.9(2)	Sn(1)−C(1)−C(2)	124.9(2)
Ge(1)−C(1)−C(6)	124.6(2)	Sn(1)−C(1)−C(6)	115.8(2)
C(1)−C(2)−C(6)	118.5(3)	C(1)−C(2)−C(6)	119.3(2)

groups on the flanking aryl rings, produced similar steric protection and also afforded crystals that diffracted X-rays readily. All four neutral compounds (ie., **1**, **2**, **8**, and **9**) displayed considerable thermal stability. The germanium compounds are a red-orange color, whereas the tin analogues form dark blue-green solutions and crystals that may also appear purple under intense illumination. The color of the compounds undergoes no apparent change when dissolved in hydrocarbons.[21] The UV−visible spectra of the germanium species feature absorbances at 371, 501 (**1**) and 365, 490 nm (**2**), whereas the corresponding wavelengths for the tin species **8** and **9** and 410, 597 and 409, 593 nm, respectively. The shift to longer wavelengths absorptions on descending a group is common in the electronic spectra of element-element bonded main group species.[22] A disappointing feature of the spectroscopic studies of the tin species **8** and **9** (and of the dianions **14**−**16**) has been our inability to detect ^{119}Sn NMR signals. Despite numerous attempts to record spectra, with use of a variety of parameters, no signals have been detected so far. We account for this in terms of the unsymmetric electron environment at tin which may cause rapid relaxation through the anisotropy of the chemical shift tensor.[23]

Data for the structures of **1** and **8** are provided in Table 2. The structure of **8** is illustrated in Figure 1. In contrast to the usually linear structure of alkynes, they possess trans-bent planar CGeGeC or CSnSnC core arrays. It can also be seen that, apart from the changed M−M distances and M−M−C angles, the structures are very similar. This similarity extends to the very low torsion angles between the central phenyl rings of the ligand and the CMMC array, only 0.4° for the germanium compound and 3.5° for the tin species. Thus, overlap of the ring orbitals of π-symmetry and a π-orbital on the dimetal units is allowed by symmetry in both cases. The Ge−C and Sn−C bond lengths, however, are not particularly short in comparison to other terphenyl substituted species. In addition, even if significantly shortened M−C bonds had been observed, it could be argued that the relatively wide M−M−C angles at germanium and tin (128.67(8)° and 125.24(7)°) afford a changed σ-hybridization which could also be a significant factor in shortening the M−C bonds.

The most important structural parameters are, of course, the trans-bending angles and the M−M distances. The M−M distances suggest the existence of considerable multiple character because they are shorter than those expected for normal single bonds between these elements (cf. 2.44 Å for germanium and 2.81 Å for tin).[24] The Ge−Ge bond length, 2.2850(6) Å, lies in the lower half of the known range (2.21−2.46 Å) for digermenes, the digermanium analogues of alkenes.[25] It is shorter than the 2.3173(3) Å observed in the digermene Ar′(Me)GeGe(Me)Ar′ [26] which has a similar degree of crowding to **1**. On the basis of the structural evidence, it can be argued that the bond order in **1** is approximately two. In contrast, the Sn−Sn bond length in **8**, 2.6675(4)Å, is less than the shortest known Sn−Sn distance in a distannene (i.e., 2.702 Å in R*(Mes)SnSn(Mes)R* (R* = $Si(SiMe_3)_3$)).[27] This should not be interpreted to imply an Sn−Sn bond order in **8** that is greater than two because most Sn−Sn bonds in distannenes are known to be quite weak, and dissociation to monomers is usually observed in hydrocarbon solutions at room temperature.[28] The Sn−Sn bond distance in **8** is slightly shorter than the 2.68(1) Å found in the tristannaallene $Sn\{Sn(SiBu^t_3)_2\}_2$[29] and is longer than the Sn−Sn double bond (2.59(1) Å) in the cyclotristannene $(Bu^t_3Si)_2SnSn(SiBu^t_3)Sn(SiBu^t_3)$.[29] On the basis of these comparisons, a bond order between 1.5 and 2.0 can be estimated for the Sn−Sn bond in **8**.

The lower bond orders in **1**, **2**, **8**, and **9** may be accounted for in terms of a second-order Jahn−Teller effect involving the mixing of a σ^* orbital and the in plane π-orbital upon trans-bending of the linear skeleton.[11,12] This can occur in heavier element compounds because the bonds are weaker, and hence, the energy separations between the bonding and antibonding levels are smaller. In this way, one of the π-orbitals associated with the M−M bonding in an idealized linear structure becomes nonbonding by mixing with a σ^* orbital upon bending the geometry, and the bond order is reduced from three to approximately two. The estimates of the bond orders and the measured structural parameters may be compared with those calculated by Bridgeman,[30] Nagase[31] and co-workers for the simple model species RMMR (M = Ge or Sn, R = H, Me, or Ph) (Table 3). For the germanium species, the Ge−Ge distance and Ge−Ge−R angle vary from 2.22 to 2.25 Å and 124°−118°, and the bond order varies from 2.32 to 1.74. For tin, the corresponding numbers are 2.65−2.67 Å, 122°−119°, and a bond order of 1.87−1.73. An independent calculation for MeGeGeMe afforded the parameters 2.197 Å, 129.7°, and a

(21) This behavior may be contrasted with that of the group 13 species Ar′GaGaAr′ which dissociates readily in solution: Hardman, N. J.; Wright, R. J.; Phillips, A. D.; Power, P. P. *J. Am. Chem. Soc.* **2003**, *125*, 2667.
(22) Tokitoh, N.; Arai, T.; Sasamori, T.; Okazaki, R.; Nagase, S.; Uekusa, H.; Okashi, Y. *J. Am. Chem. Soc.* **1998**, *120*, 443.
(23) Eichler, B. E.; Phillips, B. L.; Power, P. P.; Augustine, M. P. *Inorg. Chem.* **2000**, *32*, 5444.
(24) Wells, A. F. *Structural Inorganic Chemistry*, 5th ed.; Clarendon: Oxford, 1984; p 1279.
(25) Escudie, J.; Ranaivonjatovo, H. *Adv. Organomet.* **1999**, *44*, 113. Power, P. P. *Chem. Rev.* **1999**, *99*, 3463.
(26) Stender, M.; Pu, L.; Power, P. P. *Organometallics* **2001**, *20*, 1820.
(27) Klinkhammer, K. W. *Polyhedron* **2002**, *21*, 587. It is not known if R*(Mes)SnSn(Mes)R* is dissociated in solution however.
(28) Goldberg, D. E.; Hitchcock, P. B.; Lappert, M. F.; Thomas, K. M.; Fjelberg, T.; Haaland, A.; Schilling, B. E. R. *Dalton Trans.* **1986**, 2387. Zilm, K. W.; Lawless, G. A.; Merrill, R. M.; Millar, J. M.; Webb, G. G. *J. Am. Chem. Soc.* **1987**, *109*, 7236.
(29) Wiberg, N.; Lerner, H.-W.; Vasisht, S.-K.; Wagner, S.; Karaghiosoff, K.; Nöth, H.; Ponikwar, W. *Eur. J. Inorg. Chem.* **1999**, 1211.
(30) Bridgeman, A. J.; Ireland, L. R. *Polyhedron* **2001**, *20*, 2841.
(31) Takagi, N.; Nagase, S. *Organometallics* **2001**, *20*, 5498.

Table 3. Calculated Structural Parameters (DFT) and Bond Orders for RMMR (M = Ge or Sn; R = H, Me, Ph, or Ar*)[30,31]

	H	Me	Ph	Ar*
Ge−Ge	2.22	2.24	2.25	2.277
Ge−Ge−R	124	127	118	123.2
bond order	2.32	2.10	1.74	
Sn−Sn	2.65	2.66	2.67	2.900
Sn−Sn−R	122	124	119	111.0
bond order	1.87	1.84	1.73	

bond order of 2.017.[32] Bearing in mind the very large size difference between the model ligands and those used experimentally, we find the calculated parameters are in good agreement with the measured values and support the lower bond order implied by the trans-bent geometries. Calculations have also been carried out on the compounds Ar*MMAr* and TbtMMTbt (M = Ge or Sn, Tbt = C_6H_2-2,4,6-{$CH(SiMe_3)_2$}$_3$).[31] The calculated values for Ar*GeGeAr* (Table 3) approach the measured values for Ar′GeGeAr′ closely. For Ar*SnSnAr* however, the calculated values differ considerably. In contrast, the calculated values for TbtGeGeTbt (Ge−Ge = 2.231Å, Ge−Ge−C = 121.8°) and TbtSnSnTbt (Sn−Sn = 2.659Å, Sn−Sn−C = 122°) are both in reasonably good agreement with those found for **1** and **8**.

Monoanionic Radical Compounds. Two germanium (**3** and **4**) and four tin (**10**−**13**) derivatives containing four different monoanions have been isolated as crystalline species. Some details of their structures are given in Table 4. Representative examples of the structures are provided by the germanium compound NaAr*GeGeAr*, **3**, and the tin derivative [K(THF)$_6$][Ar′SnSnAr′], **11**, which are illustrated in Figure 1. The planarity of the core and the trans-bent geometry seen in the neutral precursors **1** and **8** are preserved in all cases. This behavior may be contrasted with that of diarylacetylenes, which, upon reduction, dimerize to form tetraarylbutadiene dianionic salts.[33] It seems likely that dimerization of the terphenyl substituted derivatives is prevented by steric effects. Within each series, the Ge−Ge and Sn−Sn distances are remarkably uniform averaging 2.32(1) Å for the germanium compounds and 2.81(1) Å for the tin species. These distances are ca. 0.03 and 0.14 Å longer than the 2.2850(6) and 2.6675(4) Å observed in neutral **1** and **8**. The other main structural change that occurs on reduction is a narrowing of the M−M−C angles. The extent of the narrowing is greatest (ca. 30°) for the tin species where an Sn−Sn−C range of 93.6(4)°−98.1(4)° is observed, cf. 125.24(7)° in the neutral Ar′SnSnAr′. For the two germanium salts **3** and **4**, the Ge−Ge−C angles are in the range 112.60(5)°−115.32(12)°, cf. 128.67(8)° in Ar′GeGeAr′, so that the amount of the closure of the Ge−Ge−C angle is less than half that seen in the tin series.

The extent of the angular change is surprising, and in the case of the tin compounds, it cannot be attributed to the effects of alkali metal countercations since similar Sn−Sn−C angles are obtained whether the alkali metal is in contact with the anion (as in **10**) or not (as in **11**−**13**). It has to be said, however, that the Na−Sn interaction in **10** is probably quite weak since the Na−Sn distance, 3.240(7) Å, is 0.14−0.17 Å longer than those observed in previously reported species with Na−Sn interactions.[27,34] Also, the data for germanium and tin series indicate that there are only minor differences between the structures of the Ar′ and Ar* derivatives. The bond length and angular changes are therefore associated with changes in the internal electronic structure that take place upon reduction of the M_2 unit. In the absence of detailed calculations on model radical species, such changes can be accounted for only in general terms. The changes probably arise from the fact that the addition of an electron to the M_2 unit effectively increases the electropositive character of the element. As a result, the electronegativity of the ligands relative to the central element is increased. By using orbital considerations and arguments similar to those used elsewhere[35,36] for the explanation of barriers to inversion or linearization in a variety of main group compounds, it can be predicted that barriers to linearization will be increased, and

Table 4. Selected Bond Distances (Å) and Angles (deg) for the Radical, Monoanion Salts NaAr*GeGeAr* (**3**), KAr′GeGeAr′ (**4**), (THF)$_3$Na{Ar*SnSnAr*} (**10**), [K(THF)$_6$][Ar′SnSnAr′] (**11**), [K(THF)$_6$][Ar*SnSnAr*] (**12**), and [K(18-crown-6)(THF)$_2$][Ar*SnSnAr*] (**13**)

NaAr*GeGeAr* (**3**)		KAr′GeGeAr′ (**4**)	
Ge(1)−Ge(2)	2.3089(8)	Ge(1)−Ge(2)	2.3331(4)
Ge(1)−C(1)	2.014(4)	Ge(1)−C(1)	2.033(2)
Ge(2)−C(37)	2.005(4)	Ge(2)−C(1)	2.036(2)
Ge(1)−Na(1)	1596(15)	Ge(1)−K(1)	3.5326(6)
Ge(2)−Na(1)	1391(15)	Ge(2)−K(1)	3.6091(6)
Na−C (range)	2.822(4)−2.981(4)	K−C (range)	3.029(3)−3.302(2)
C(1)−Ge(1)−Ge(2)	114.2(1)	C(1)−Ge(1)−Ge(2)	115.55(5)
C(37)−Ge(2)−Ge(1)	115.3(1)	C(31)−Ge(2)−Ge(1)	112.59(5)
Ge(1)−C(1)−C(2)	124.8(3)	Ge(1)−C(1)−C(2)	120.18(16)
Ge(1)−C(1)−C(6)	117.5(3)	Ge(1)−C(1)−C(6)	122.96(15)
C(2)−C(1)−C(6)	116.8(4)	C(2)−C(1)−C(6)	116.24(19)
Ge(2)−C(37)−C(38)	117.2(3)	Ge(2)−C(31)−C(36)	124.09(17)
Ge(2)−C(37)−C(42)	125.0(3)	Ge(2)−C(31)−C(36)	119.55(17)
C(38)−C(37)−C(42)	116.7(4)	C(32)−C(31)−C(36)	115.9(2)
[K(THF)$_6$][Ar′SnSnAr′] (**11**)		[K(THF)$_6$][Ar*SnSnAr*] (**12**)	
Sn(1)−Sn(1A)	2.8081(9)	Sn(1)−Sn(1A)	2.8123(9)
Sn(1)−C(1)	2.249(6)	Sn(1)−C(1)	2.236(5)
K(1)−O(1)	2.623(7)	K(1)−O(1)	2.684(7)
K(1)−O(2)	2.703(9)	K(1)−O(2)	2.7003(6)
		K(1)−O(3)	2.684(7)
C(1)−Sn(1)−Sn(1A)	97.91(16)	C(1)−Sn(1)−Sn(1A)	95.20(13)
Sn(1)−C(1)−C(2)	120.9(3)	Sn(1)−C(1)−C(2)	120.2(4)
C(2)−C(1)−C(2A)	117.5(6)	Sn(1)−C(1)−C(6)	123.0(4)
		Sn(1)−C(2)−C(6)	116.6(5)
[(THF)$_3$Na{Ar*SnSnAr*}] (**10**)		[K(18-crown-6)(THF)$_2$][Ar*SnSnAr*] (**13**)	
Sn(1)−Sn(2)	2.8107(13)	Sn(1)−Sn(1A)	2.782(1)
Sn(1)−C(1)	2.22(2)	Sn(1)−C(1)	2.29(1)
Sn(2)−C(37)	2.19(1)	Sn(2)−Sn(2A)	2.824(1)
Na(1)−Sn(1)	3.240(7)	Sn(2)−C(2)	2.226(7)
Na(1)−O(1)	2.26(2)	C(1)−Sn(1)−Sn(1A)	95.0(4)
Na(1)−O(2)	2.35(2)	C(1A)−Sn(1)−Sn(1A)	93.6(4)
Na(1)−O(3)	2.47(2)	C(37)−Sn(2)−Sn(2A)	97.3(2)
C(1)−Sn(1)−Sn(2)	97.9(3)		
C(37)−Sn(2)−Sn(1)	98.0(4)		
C(1)−Sn(1)−Na(1)	131.3(4)		
Sn(2)−Sn(1)−Na(1)	130.4(2)		
Sn(1)−C(1)−C(2)	121(1)		
Sn(1)−C(1)−C(6)	125(1)		
C(2)−C(1)−C(6)	114(1)		

(32) Allen, T. L.; Fink, W. H.; Power, P. P. *J. Chem. Soc., Dalton Trans.* **2000**, 407.
(33) Schlenk, W.; Bergman, E. *Justus Liebigs Ann. Chem.* **1928**, *463*, 71. Smith. L. I.; Hoehn, H. H. *J. Am. Chem. Soc.* **1941**, *61*, 1184.
(34) Klinkhammer, K. W. *Chem.—Eur. J.* **1999**, *3*, 1418. Wiberg, N.; Lerner, H.-W.; Wagner, S.; Nöth, H.; Seifert, T. *Z. Naturforsch* **1999**, *54b*, 877.
(35) Levin, C. C. *J. Am. Chem. Soc.* **1975**, *97*, 5649.
(36) Gilheany, D. G. *Chem. Rev.* **1994**, *94*, 1339.

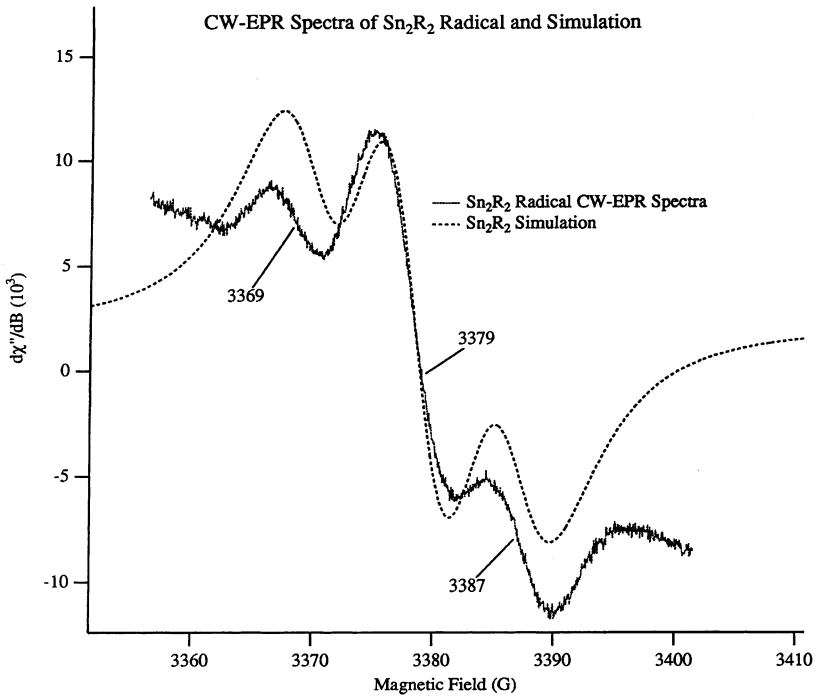

Figure 2. EPR spectrum of a ca. 0.1 mM solution of $[K(THF)_6][Ar^*SnSnAr^*]$ in THF at 296 K.

the interligand angles decreased, by the addition of an electron to the M_2 unit. This effect is greatest in tin since the electronegativity differences between the metal and ligand are larger. The narrower M−M−C angles in the radicals probably also give rise to an increase in the p-character of the σ-bonds.[37] This is expected to lead to longer bond lengths as a result of the greater average radius of the p-orbitals vis-à-vis s-orbitals. The longer Ge−C, Sn−C, Ge−Ge, and Sn−Sn bonds experimentally observed in the radicals are in agreement with this hypothesis. In addition, the character of the orbital to which the electron has been added is also of prime importance for the M−M bond lengths. Calculations on the model germanium and tin compounds MeGeGeMe[32] and MeSnSnMe[38] show that the LUMO resembles an n_+ lone pair combination and not the π^*-orbital observed for alkynes. The LUMO appears to be mainly nonbonding in character (although it also has a small component between the M nuclei) so that the addition of an electron to it is expected to have a small effect on the M−M distance. These results suggest that the lengthening of the M−M and C−C bonds that occur on single-electron reduction is largely a result of σ-bonding effects.

The energy level order within the monoanions in **3**, **4**, and **10**−**13** or their model species is currently unknown, but the near 90° Sn−Sn−C angle in the tin monoanions could be accompanied by a change in the ordering of the energy levels associated with the M_2 unit. Thus, when the M−M−C bond angle is narrowed from 180° to ca. 90°, the bonding is changed from triple to approximately single as shown by the schematic

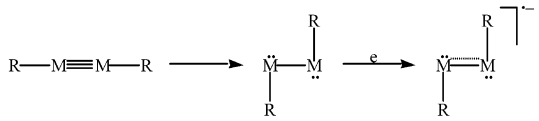

This leaves an unused p-orbital at each M which lie perpendicularly to the CMMC plane. If it is assumed that a combination of these two p-orbitals is the LUMO, the addition of an electron generates a π-bond of order 0.5 to yield an M−M bond of order 1.5. The Sn−Sn bonds in the reduced, monoanionic species **10**−**13** are close to the Sn−Sn distance in elemental (gray) tin[24] which suggests little multiple character. However, as discussed above, it is probable that the multiple character and shortening of the Sn−Sn bond be masked by the lengthening of the σ-bond due to the closure of the Sn−Sn−C angle. This view receives support from the structure of the neutral lead compound $Ar^*PbPbAr^*$[5,37] which has a Pb−Pb σ-bond, a Pb−Pb−C angle of 94.26(4)°, and a "long" Pb−Pb bond length of 3.188(1) Å which is ca. 0.30 Å longer than a "normal" Pb−Pb single bond in R_3PbPbR_3 species (e.g., 2.844(4) Å in $Ph_3PbPbPh_3$).[39]

The EPR spectrum of **12** in THF at room temperature displayed a strong signal near $g = 2.0691$ with hyperfine coupling to ^{117}Sn ($I = {}^1/_2$, 7.68%) and ^{119}Sn ($I = {}^1/_2$, 8.58%). Simulation of the spectrum afforded a(^{117}Sn) and a(^{119}Sn) couplings of 8.3 and 8.5 G (Figure 2), although the difference between the couplings was not resolved in the experimental spectrum. More recent work on the germanium radical **4** afforded a signal centered near $g = 2.003\,82$ with a hyperfine coupling to ^{73}Ge ($I = {}^9/_2$, 7.8%) of 7.5 G. The small coupling constants in both compounds suggest very low unpaired electron density at the germanium or tin nuclei. Cyclic voltammetric studies of **8** in THF revealed a facile, essentially reversible redox cycle at −1.21 V versus SCE (Figure 3). On the other hand, the germanium species **1** displayed an irreversible reduction wave at ca. −1.38 V. No other reduction waves could be observed until solvent breakdown occurred near −2.4 V. Although **8** and **9** (like **1** and **2**) can be doubly reduced, it seems

(37) It is not possible to deduce the extent of hybridization from bond angles. However, in the related species $Ar^*PbPbAr^*$[5] which has a Pb−Pb−C bond angle that approaches 90°, the extent of hybridization is low: Chen, Y.; Hartmann, M.; Diedenhofen, M.; Frenking, G. *Angew. Chem., Int. Ed.* **2001**, *40*, 2052.
(38) Phillips, A. D.; Power, P. P. Unpublished work.
(39) Preut, H.; Huber, F. *Z. Anorg. Allg. Chem.* **1976**, *419*, 92−96.

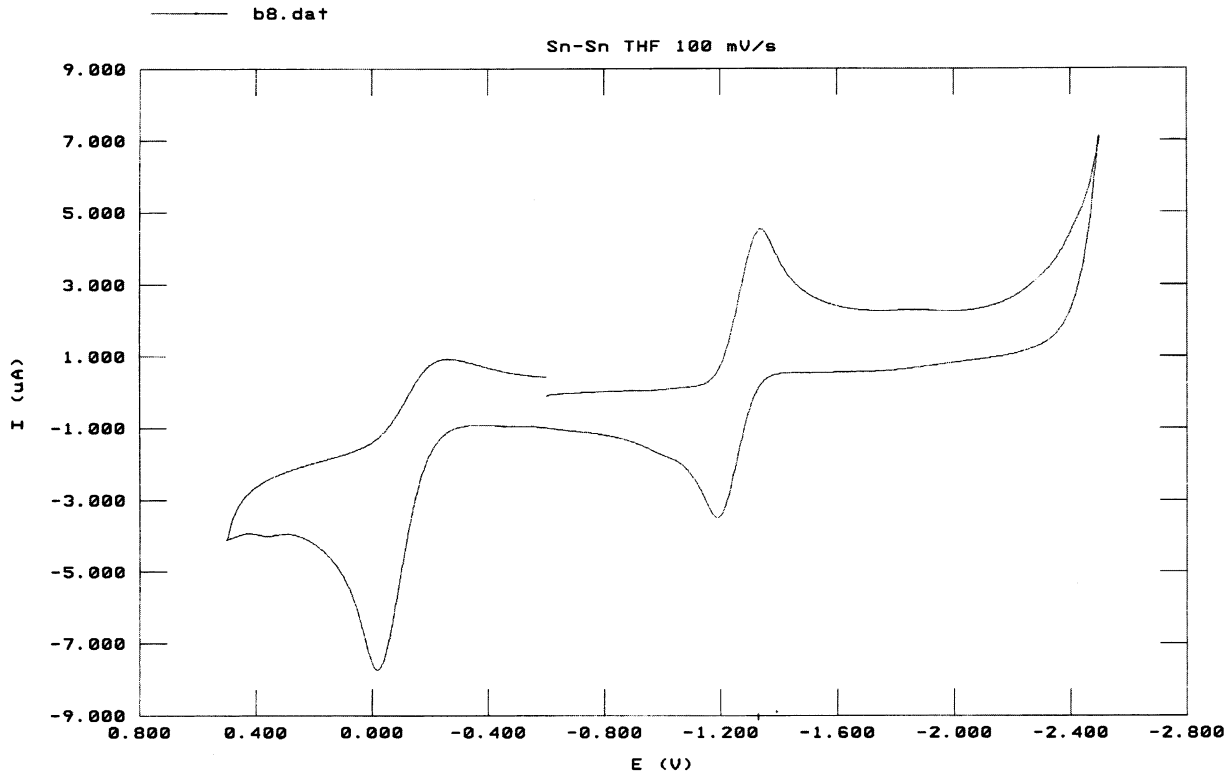

Figure 3. Cyclic voltammogram of ca. 1 mM Ar′SnSnAr′ (**8**) in 0.1 M tetrabutylammonium perchlorate in THF referenced to SCE and scanned at 100 mV s^{-1}.

Table 5. Selected Bond Distances (Å) and Angles (deg) for the Dianionic Salts Li_2Ar′GeGeAr′ (**5**), Na_2Ar*GeGeAr* (**6**), K_2Ar*GeGeAr* (**7**), Na_2Ar*SnSnAr* (**14**), K_2Ar′SnSnAr′ (**15**), and K_2Ar*SnSnAr* (**16**)

Li_2Ar′GeGeAr′ (**5**)		Na_2Ar*GeGeAr* (**6**)		K_2Ar*GeGeAr* (**7**)	
Ge(1)−Ge(1A)	2.455(9)	Ge(1)−Ge(1A)	2.394(1)	Ge(1)−Ge(1A)	2.3912(6)
Ge(1)−C(1)	2.060(3)	Ge(1)−C(1)	2.065(3)	Ge(1)−C(1)	2.077(3)
Ge(1)−Li(1)	2.874(6)	Ge(1)−Na(1)	3.121(2)	Ge(1)−K(1)	3.5573(8)
Ge(1)−Li(1A)	2.892(7)	Ge(1)−Na(1A)	3.074(3)		
Li−C (range)	2.482(7)−2.759(7)	Na−C (range)	2.049(3)−2.831(3)	K(1)−C (range)	3.027(3)−3.179(3)
C(1)−Ge(1)−Ge(1A)	102.97(9)	C(1)−Ge(1)−Ge(1A)	102.37(8)	C(1)−Ge(1)−Ge(1A)	112.14(7)
Ge(1)−C(1)−C(2)	121.8(2)	Ge(1)−C(1)−C(2)	122.5(2)	Ge(1)−C(1)−C(2)	122.3(2)
Ge(1)−C(1)−C(6)	122.3(2)	Ge(1)−C(1)−C(6)	121.7(2)	Ge(1)−C(1)−C(6)	120.7(2)
C(2)−C(1)−C(6)	115.1(3)	C(2)−C(1)−C(6)	114.9(2)	C(2)−C(1)−C(6)	113.9(2)
Na_2Ar*SnSnAr* (**14**)		K_2Ar′SnSnAr′ (**15**)		K_2Ar*SnSnAr* (**16**)	
Sn−Sn′	2.789(1)	Sn(1)−Sn(1A)	2.7754(3)	Sn−Sn′	2.7763(9)
Sn−C(1)	2.249(9)	Sn−C(1)	2.282(2)	Sn−C(1)	2.274(6)
Na(1)−Sn	3.298(5)	K(1)−Sn(1)	3.5947(5)	K(1)−Sn	3.579(2)
Na(2)−Sn	3.309(5)	K(1A)−Sn(1)	3.6383(5)	K(2)−Sn	3.591(2)
Na−C (range)	2.934(9)−3.084(9)	K−C (range)	3.097(2)−3.227(2)	K−C (range)	3.076(7)−3.247(7)
Sn′−Sn−C(1)	104.8(2)	Sn(1A)−Sn(1)−C(1)	106.02(5)	Sn′−Sn−C(1)	107.5(1)
Sn−C(1)−C(2)	121.7(8)	Sn(1)−C(1)−C(2)	121.3(1)	Sn−C(1)−C(2)	120.9(5)
Sn−C(1)−C(6)	120.8(8)	Sn(1)−C(1)−C(6)	121.3(1)	Sn−C(1)−C(6)	120.9(5)
C(2)−C(1)−C(6)	115.6(8)	C(2)−C(1)−C(6)	115.1(2)	C(2)−C(1)−C(6)	115.6(5)

probable that the resultant dianion is only stable in the presence of contact alkali metal cations. These cations are unavailable in the CV solutions of neutral **1** or **8** in THF. The more facile reduction of the tin compound supports the view that the LUMO in this molecule lies lower than that in the germanium species which is consistent with weaker bonding in the tin species.

Doubly Reduced Compounds. The reaction of Ar′MCl or Ar*MCl (M = Ge or Sn) with excess lithium, sodium, or potassium for extended periods afforded the doubly reduced compounds **5**−**7** and **14**−**16**. The syntheses of **6** and **16** were described in a preliminary publication.[9] A range of compounds with different alkali metals and aryl substituents was investigated in order to gauge the effect of the various countercations and the two aryl groups on the structures. The structural results are summarized in Table 5. Trans-bent, planar CMMC cores were observed in all cases. In addition, all the compounds are contact ion triples in which the two alkali/metal countercations are sandwiched between flanking aryl rings, each of which is drawn from a different terphenyl group. The alkali metal cations bridge the two germanium or tin atoms in an almost symmetric manner and form a planar array with the germanium or tin atoms that is perpendicular to the CMMC plane. It can be seen that the use of sodium or potassium countercations affords structures with Ge−Ge or Sn−Sn and Ge−C or Sn−C distances that are

very similar. The only notable differences between the sodium and potassium salts, besides the alkali metal-germanium, tin, or carbon distances, are the M−M−C angles. Wider M−M−C angles are observed for the potassium derivatives, most notably for the germanium species **6** and **7** where the difference is ca. 10°. The larger size of the K^+ ions, which are complexed to the aryl rings, probably causes the wider M−M−C angles. The K−C distances in **7**, **15**, and **16** are comparable to each other, but the Na−C distances in the germanium salt **6** are shorter than those in its tin analogue **14** which suggests that Na^+ is too small for the cavity between the aryl rings in **14**. The Na−Sn distance in **14** is close to that observed in the monoanion **10**. Furthermore, the Na−Ge and K−Ge distances in **6** and **7** are very similar to those in the monoanionic derivatives **3** and **4**.

When the Ge−Ge distances in **5**−**7** and the Sn−Sn distances in **14**−**16** are compared to those in the monoanions, it can be seen that the Ge−Ge distances increase from ca. 2.32 to ca. 2.39 Å, whereas the Sn−Sn distances decrease slightly from ca. 2.81 to ca. 2.78 Å. Furthermore, the Ge−Ge−C angles in **6** and **7** are narrower than those in the monoanions **3** and **4**, whereas the Sn−Sn−C angles in **14**−**16** are wider than those in monoanions **10**−**13**. The shorter Sn−Sn bond lengths, although consistent with the addition of another electron to an Sn−Sn π-orbital, can also be explained through the widening of the Sn−Sn−C angle which could cause bond shortening by σ-effects. Furthermore, the increase in Coulombic repulsion that occurs upon the addition of the second electron may be not as great as it is in the germanium system due to the relatively large size of the tin. The Ge−Ge bond length increase that occurs upon further reduction of the germanium compounds is consistent with the addition of the second electron to the n_+ LUMO. The further narrowing of the Ge−Ge−C angle, owing to the increasing relative electropositive character of the germanium, combined with the increase in Coulombic repulsion, produces a significant bond length increase to ca. 2.39 Å.

The structure of the dilithium salt **5** resembles that of the sodium salt **6** in having almost equal trans-bending angles and Ge−C bond lengths. As expected, the Li−Ge and Li−C distances are shorter than the corresponding Na−Ge and Na−C distances owing to the smaller size of lithium. The Li−C distances span an almost identical range to those seen in the structures of $(LiSC_6H_2\text{-}2,4,6\text{-}Ph_3)_4$ and $(LiSC_6H_3\text{-}2,6\text{-}Mes_2)_3$.[40] In contrast, the Ge−Ge bond length in **5** (2.457(2) Å), which is ca. 0.06 Å longer than those observed for **6** and **7**, was less predictable. The Li−Ge distances (two shorter at ca. 2.83 Å and two longer at ca. 2.94 Å) lie at the high end of the currently known range.[41,42] Normally, Li−Ge distances lie within ca. 2.55−2.75 Å,[41] but an unusually long Li−Ge distance, 2.904-(12) Å, has been found in $[(THF)_3LiGe\{N(Ph)SiMe_2O\}_3\text{-}SiBu^t]$.[42] These data suggest a relatively weak interaction between lithium and germanium. Despite this, the small size and high polarizing power of the Li^+ ion may cause the lengthening in the Ge−Ge bond by attracting electron density toward itself from the π-bonds. Calculations at the B3LYB/6-31 level confirm longer Ge−Ge bonds with Li countercations.[38] Such effects have been calculated for other systems that involve alkali metal salts of dianionic systems.[43,44] Finally, it is notable that the dianions $[Ar'MMAr']^{2-}$ and $[Ar^*MMAr^*]^{2-}$ (M = Ge or Sn) are isoelectronic to the corresponding neutral arsenic and antimony species, Ar*PnPnAr* (Pn = As or Sb), which have As−As and Sb−Sb double bonds.[45]

Conclusions

It has been shown that large terphenyl ligands stabilize germanium and tin analogues of alkynes. These have decreased Ge−Ge and Sn−Sn bond orders that are less than three due to the electronic properties of the Ge−Ge and Sn−Sn units which permit mixing of a σ*- and a π-level and consequent transformation of a π-level into an n_- lone pair combination. The compounds can be easily reduced to mono- or dianionic species. Reduction by one electron affords narrower trans-bending angles and increased Ge−Ge and Sn−Sn bond lengths. The addition of another electron further increases the Ge−Ge bond distance but shortens the Sn−Sn bond slightly. These trends have been rationalized on the basis of the character of the molecular orbitals likely to be involved in M−M bonding. Further evidence of the nature of the M−M bonds will come from the reaction chemistry of the compounds themselves.

Acknowledgment. We are grateful to the National Science Foundation (CHE-0096913) for financial support. We thank Prof. T. L. Allen and W. H. Fink for useful discussions and Prof. F. Osterloh for his essential help in recording the electrochemical data.

Supporting Information Available: X-ray data (CIF) for Ar′GeCl and Ar′SnCl, **3**−**5**, **7**, **11**, **14**, and **15**. This material is available free of charge via the Internet at http://pubs.acs.org.

JA035711M

(40) Niemeyer, M.; Power, P. P. *Inorg. Chem.* **1996**, *35*, 7264.

(41) West, R.; Sohn, H.; Powell, D. R.; Muller, T.; Apeloig, Y. *Angew. Chem., Int. Ed. Engl.* **1996**, *35*, 1002. Hong, H.-H.; Pan, Y.; Boudjouk, P. *Angew. Chem., Int. Ed. Engl.* **1996**, *35*, 186. Freitag, D. S.; Herbst-Irmer, R.; Lameyer, L.; Stalke, D. *Organometallics* **1996**, *15*, 2838. Hitchcock, P. B.; Lappert, M. F.; Layh, M. *Chem. Commun.* **1998**, 2179. Kawachi, A.; Tanaka, Y.; Tamao, K. *Eur. J. Inorg. Chem.* **1999**, 461. Choi, S.-B.; Boudjouk, P.; Hong, H.-H. *Organometallics* **1999**, *18*, 2918. Choi, S.-B.; Boudjouk, P.; Qin, K. *Organometallics* **2000**, *19*, 1806. Dysard, J. M.; Tilley, T. D. *J. Am. Chem. Soc.* **2000**, *122*, 3097. Habereder, T.; Nöth, H. *Z. Anorg. Allg. Chem.* **2001**, *627*, 1003.

(42) Veith, M.; Schutt, O.; Huch, V. *Angew. Chem., Int. Ed.* **2000**, *39*, 601.

(43) Takagi, N.; Schmidt, M. W.; Nagase, S. *Organometallics* **2001**, *20*, 1646.

(44) Phillips, A. D.; Power, P. P. *J. Cluster Sci.* **2002**, *13*, 569.

(45) Twamley, B.; Sofield, C. P., Olmstead, M. M.; Power, P. P. *J. Am. Chem. Soc.* **1999**, *121*, 3357.